Fretting wear of alloy steels at the blade tip of steam turbines

Fretting wear of alloy steels at the blade tip of steam turbines

M. Lavella* (1), D. Botto (1)
(1) Department of Mechanical and Aerospace Engineering, Politecnico di Torino Corso Duca degli Abruzzi, 24-10129 Torino – Italy

Received Date Line (to be inserted by Production) (8 pt)

Abstract

In order to reduce blade resonant vibration amplitude in turbomachinery, blades are assembled with a mutual interlocking at the tip. The aim of this study is to investigate the wear mechanism at the contact interface of the blade shroud in steam turbines. Experimental data are available concerning the wear mechanism at interfaces of aircraft engines blades, while the literature regarding the same effect on steam turbines is less rich. Moreover, the transposition of the results from the aero engine to the steam turbine is difficult, because materials and working conditions are different. To overcome this lack of knowledge an experimental campaign was set up to investigate this wear mechanism under the specific conditions and with the distinctive materials used in steam turbines.

Two base materials (alloy steels) were tested under different conditions: surface treatment (with and without laser quenching), temperature and normal load. Dissipated energies were determined from the hysteresis loops measured during the tests and were correlated to the test conditions. Profiles of worn surfaces were measured, and volume losses were accurately computed with a procedure that takes into account the roughness of the surfaces.

Experiments were conducted both at room and low temperature (150 °C). At room temperature the surface temperature increased to 60-70 °C, due to the heat generated in the wear process. Comparison of volume losses at room and low temperature showed that at 150°C the volume losses decreased dramatically. This behaviour was explained with a brittle-ductile transition. In other words, the same wear mechanism, adhesion and abrasion respectively in stick and gross slip condition, give very different results for a small softening effect of the material. Moreover, experimental results showed much more sensitive wear rates to the heat treatment than to the steel type.

Keywords: fretting, wear, M152 steel, X20Cr13 steel, steam turbine, brittle-ductile transition.

*Corresponding author. Tel.: +39 011 0906935; fax: +39 011 0906999.
E-mail address: mario.lavella@polito.it (Mario Lavella)

1. Introduction

Steam turbines are used as drivers of electrical generators, oil refinery, naval propulsion and many others important applications. Steam turbines cover a very wide variety of sizes (from hundreds of kW to many GW) and configurations. As electrical energy is mainly generated by steam turbines, breakdowns are detrimental for the economy. These applications are usually strategic for life and safety. Maintenance programmes are carefully scheduled to evaluate the integrity of turbomachinery components, particularly of the blades, to decrease breakdown risks in turbines. On the other hand, the steam turbine industry aims to increase the maintenance interval, to reduce the turbine out-service time. High cycle fatigue cracks in blades are nucleated and propagated by turbine vibrations [1] that increase displacement amplitude of the blade and related stress. Consequently, the identification techniques are continuously developed in order to better characterize blade vibrations [2]. Fillets at the blade root and eroded wear zones are typical sites of crack nucleation. For this reason many studies have been published to better understand the failure mechanism by erosion wear in steam turbine blades [3]-[7].

A widely used method to reduce displacement amplitude of the blade is to increase the internal damping of the blade assembly. This is done by introducing under-platform dampers, that are devices placed close to the blade shank. These devices dissipate part of the vibrational energy in the contact between the damper and the blade platform [8]-[10]. A different way to decrease the amplitude displacement of blades is to increase the stiffness of the assembly. Blades are fit with interference with the neighbouring blades. Interference fit, also denoted as “interlocking”, is usually given at the blade tip where a shroud is machined. If vibrations generate excessive relative displacement of adjacent blades, wear occurs at the contact surface of the shrouds and causes loss of interlocking. Diminished interlocking decreases the assembly stiffness and then is less effective in reducing amplitude displacement of the blades. This condition triggers a loop that could lead to catastrophic failure. Consequently, to improve the dynamic design of the bladed disk and to schedule appropriate maintenance intervals, knowledge of the contact parameters (friction coefficient and contact stiffness), wear mechanisms and wear evolution are of paramount importance.

In the gas turbine, blade failure is commonly mitigated by reducing the vibration amplitude of the blade using dampers and shrouds. Recently this strategy is also applied to the steam

turbine. These interfaces have already been studied for aircraft engines: some examples are [11]-[13]. As the materials and the service condition of the aircraft engines are different, the results obtained cannot be transferred to steam turbine.

This paper shows the methodology and the results of an experimental campaign performed to investigate the wear mechanism and wear evolution of the typical materials used for blades in low-pressure stages in steam turbines. Test parameters were representative of the typical operating conditions. High-precision test rig [14]-[15] with free approach of flat on flat contact surfaces was used in order to have a rigorous measurements of wear evolution. These fretting experiments are not affected by imprecisions due to the assembling-reassembling of specimens and test rig compliance. Assembling-reassembling operations are necessary for the topological measurements of the contact surface. The test rig compliance affects the relative displacement measurements introducing a difference between imposed and real displacement amplitude. Wear volume measurements was performed considering the roughness of the contact surfaces. Novel interpretations in terms of surface integrity and brittle-ductile transition of the oxides layers on contact interfaces was proposed.

2. Methods and materials

The tribological properties of low pressure shroud blades for steam turbine applications were evaluate by means of experimental fretting tests. The fretting wear on these mating surfaces, see Fig. 1, is generate by the blade vibrations.

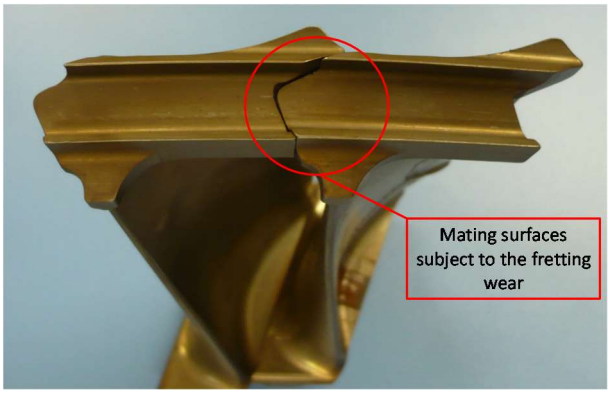

Fig. 1. Fretted mating surfaces at blade tip.

Fretting tests were performed by means of the test rig illustrated in Fig. 2. All the characteristic of test rig can be found in [14].

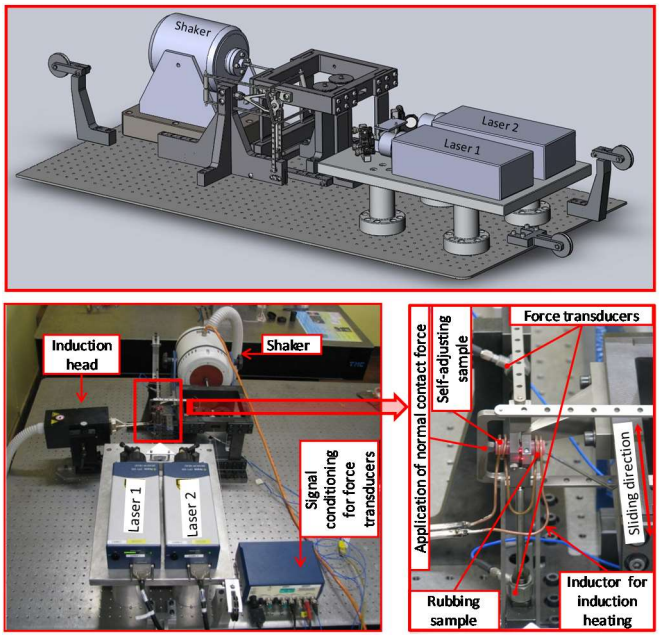

Fig. 2. Test rig.

The main peculiarities of this test rig are: flat on flat contact with free approaching of contact surfaces; displacement control; contact force and relative displacement measured continuously for each hysteresis loop; working temperature from Room Temperature (RT) to 1000 °C. The relative displacement are measured and very near to the contact interfaces, substantially there is no difference between the imposed sliding amplitude and the applied amplitude, about the importance of imposed and applied sliding amplitude [16]. In other words, there are no effect of test rig compliance on the displacement measurements [17]. Moreover, because of the free approaching and the fixture specimen's characteristic, the test rig allows the disassembling and subsequent re-assembling with a negligible impact on the fretting process. Disassembling – assembling operations are necessary to measure the 3D profile of the worn surfaces and to determine the wear volume. A great advantage of this rig is that wear volume measurements can be done on the same couple of specimens at different stage of the fretting process.

The geometry of specimens is shown in Fig. 3. Two sliders, symmetrically located with respect to the specimen centre, are machined on the specimen mounted on the fixed support. The specimen was assembled with the slider longitudinal axis parallel to the sliding direction. The length of contact surfaces measured along the sliding direction was 5.4 mm while the width of the contact surfaces measured along the orthogonal direction was 1 mm, Fig. 3. The specimen mounted on the mobile support had only one contact surface. The length of this contact surface measured along the sliding direction was the same of the slider (5.4 mm). This design condition allows to avoid the impact with the groove edge at the inversion motion points. Consequently, even the strain hardening effect at the inversion points of the hysteresis loops is avoided [11].

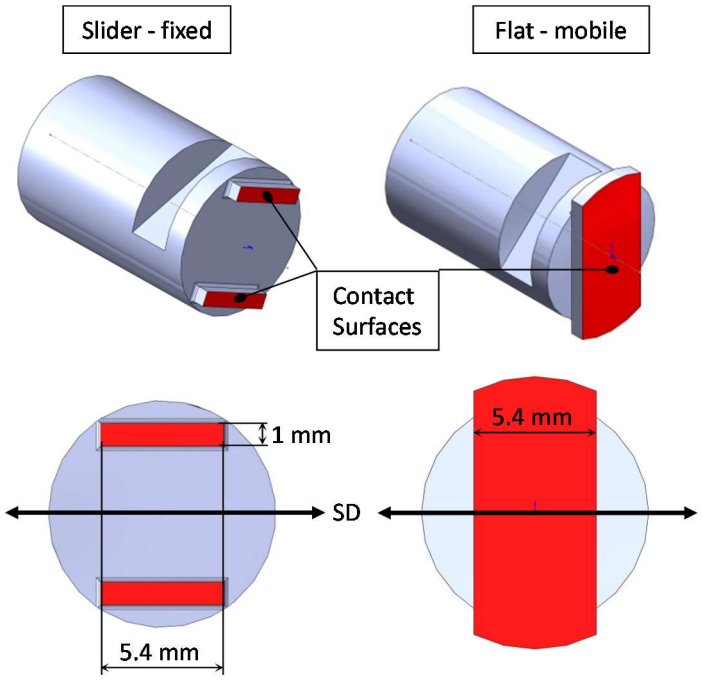

Fig. 3. Fixed and mobile sample: SD Sliding Direction; length of contact surfaces measured along the sliding direction 5.4 mm, width of contact surfaces measured in the direction orthogonal to the sliding direction 1 mm.

The pressure distribution for a given normal load and the relative displacement associated to a tangential load can be simulated using the method proposed in [18]. In this method, a reduced order model is obtained from a full finite element model using a static reduction. The sliders give two nominally equal pairs of contact surfaces. Each pair had a surface 5.4 mm^2 while the overall contact surface of the couple of specimens was 10.8 mm^2. These two pairs of contact surface

ware subject to the same fretting process but wear volume was measured independently to have one repetition of the fretting process.

Experiments ware performed to investigate some alternative for the blade tip shrouds of steam turbine at stages L-2, L-1, L-0. Effects of material, heat treatment, normal load, and temperature were analysed. Particularly, tests were performed on two stainless steels (M152 and X20Cr13), two heat treatments (quenching – tempering with and without laser quenching), two nominal contact pressures (25 and 15 MPa), two temperatures (RT and 150 °C), one stroke (50 μm), one frequency (175 Hz). The durations of the wear process were 25×10^6 cycles for all tests except two which had a duration of 15×10^6 cycles. Each wear test was divided in stint of 5×10^6 wear cycles and the worn surfaces profiles were evaluated at the end of each stint. Worn volumes were computed using the topographic measurements of contact surfaces, measured in unworn condition, and after 5×10^6, 10×10^6, 15×10^6, 20×10^6, 25×10^6 wear cycles.

The wear volume was evaluated with a procedure that considers the roughness of the mating surfaces [13]. It was measured by comparison of peaks and holes volume measurements of asperities at different steps of fretting process starting from unworn conditions. Peak and hole volumes was defined using a reference plane which was set by means of last square interpolation of unworn area. Consequently, a positive wear volume is obtained if the sum of peaks volumes decreases and the sum of holes volumes increases. In the case of the slides, the comparison was made using the entire volume of one slider at each step of the wear process. Each slider and the relative contact surface on the flat sample was evaluate without any influence of the other slider. This strategy was used in order to evaluate the repeatability of the measurements on each couple of contact surfaces.

During the fretting processes the relative displacement and the tangential contact force were measured and stored. The tangential contact force plotted against the relative displacement gives the hysteresis loop. The contact parameters, namely friction coefficient and contact stiffness, were obtained by post-processing hysteresis loops. The area of the hysteresis loop is the energy dissipated during a fretting cycle. In this work, the dissipated energy at each loops acquisition was evaluated measuring by integration the areas on the hysteresis loops acquired during fretting process. Twenty loops were stored per each acquisition. These loops were used for computing an average dissipated energy [13], [14] characteristic of the specific acquisition. The total dissipated energy losses at a specific cycle during the fretting process is the sum of the energy

dissipated par each cycle from the first. Due to the huge amount of data, loops were not stored continuously over the fretting process. As an acceptable alternative, the hysteresis loops were stored after a pre-planned number of cycles. The sum of dissipated energies were based on the average energies computed at each loops acquisitions. Between two subsequent loop acquisitions the dissipated energy for each cycle were obtained by linear interpolation. The loops data acquisitions were performed every 0.25×10^6 cycles. During the beginning, before 0.25×10^6 cycles and the end a wear stage ($4.75 \times 10^6 \div 5 \times 10^6$ cycles) the acquisitions were more frequent.

3. Results and discussion

The detailed experimental plan is reported in Table 1. It details normal loads, materials, heat treatment, and test temperature. Fig. 4 illustrates the wear volume as a function of wear cycles for M152 and X20Cr13 steels at RT. The wear volume was obtained as the sum wear volume measured on both mating surfaces. There are two measurements of wear volumes for each number of cycles because of the two sliders. The wear volume relation as a function of wear cycles shows a linear evolution with a good repeatability.

Table 1: experimental plan.

ID couple	Material	Heat treating	Temp, C	Normal Load, N	Contact Pressure, MPa (1)	Cycles, ($\times 10^6$)
#01-M152	M152	Q-T	RT	271.8	25	25
#02-M152	M152	Q-T-LQ	RT	271.8	25	25
#03-X20Cr13	X20Cr13	Q-T	150	271.8	25	25
#04-X20Cr13	X20Cr13	Q-T-LQ	150	271.8	25	25
#05-X20Cr13	X20Cr13	Q-T	RT	271.8	25	25
#06-M152	M152	Q-T	RT	271.8	25	25
#09-X20Cr13	X20Cr13	Q-T	RT	163.7	15	15
#10-M152	M152	Q-T	RT	163.7	15	15

Common data and abbreviations:

Stroke: 50 µm
Frequency: 175 Hz
Q-T: Quenching and Tempering;
Q-T-LQ: Quenching, Tempering and Laser Quenching;
Temp: Temperature
RT: Room Temperature
(1) Nominal value Normal load/Contact surface

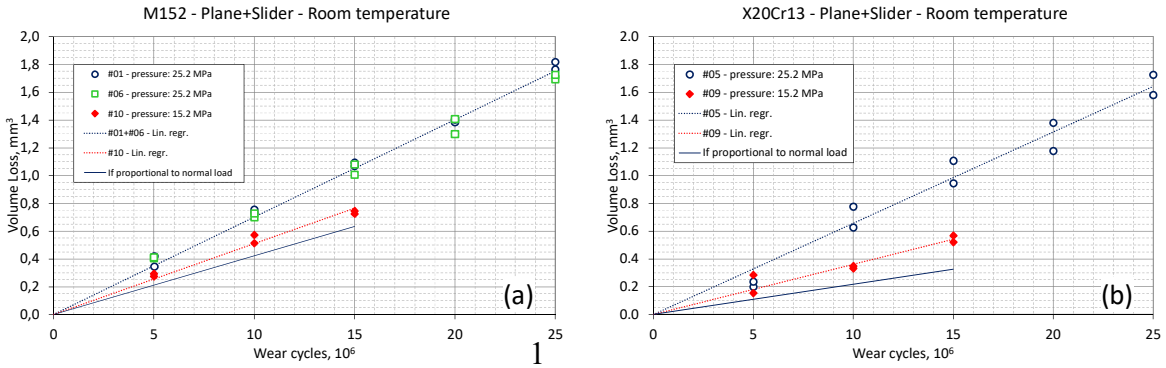

1

2

3 Fig. 4. Effect of normal load, wear volume as a function number of wear cycles for two normal loads: (a) M152;
4 (b) X20Cr13.

5

6 This linear relation has a lower slope at lower normal load. Moreover, the slope at lower normal
7 load is higher than the slope of a linear law where the wear volume is proportional to the normal
8 load (see continuous lines in Fig. 4). This difference of slope is confirmed for both materials and
9 have a similar magnitude. These results suggest that, in general, there is no a linear relation
10 between wear volume and normal load. Consequently, the specific wear volumes obtained at a
11 specific normal load cannot be extended to other normal load using linear law.

12 A different dependence between wear volume and normal load can be obtained from the plot
13 of relations wear volume as a function of the dissipated energy during the fretting process. Fig.
14 5 reports the same wear volume of Fig. 4 as a function of dissipated energy.

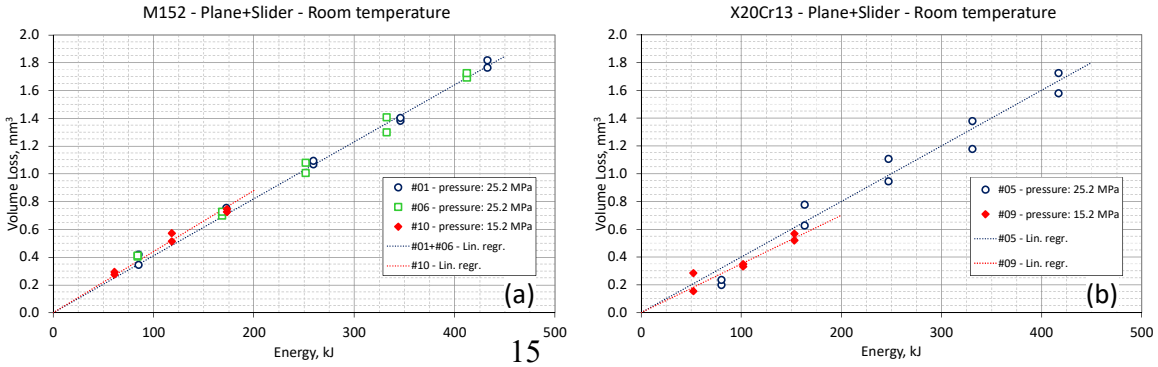

15

16

17 Fig. 5. Effect of normal load, wear volume as a function dissipated energy for two normal loads: (a) M152; (b)
18 X20Cr13.

19

The relation between wear volume and dissipated energy is linear similarly to the relation between volume and cycles, but the variation due to the different normal load is much less evident. Moreover, the difference of slope is slightly higher at lower normal load for M152 (Fig. 5 (a)) while it is slightly lower at lower normal load for the X20Cr13 (Fig. 5 (b)). This result suggests that the relation between wear volume and dissipated energy is independent from the normal load. As a consequence, experiments at low normal load can be included in the same volume – energy relation of those at higher normal load. The difference of the higher – lower normal load slopes can be attributed to unavoidable measurement errors. The fretting regimes of these tests were gross slip.

The influence on the wear rate of materials and heat treatment at RT is summarized in Fig. 6. This figure reports wear volume as a function of dissipated for M152 with and without laser quenching and X20Cr13 at RT. These results indicate that the wear rate is more influenced from the heat treatment than from the material. The X20Cr13 shows a wear rate lower than that of the M152. On the other hand, the effect of the surface laser quenching on the X20Cr13 revels lower wear rates than the difference observed by comparison of two steels without surface heat treatment. Thus, the beneficial effect of the laser quenching is evident at RT.

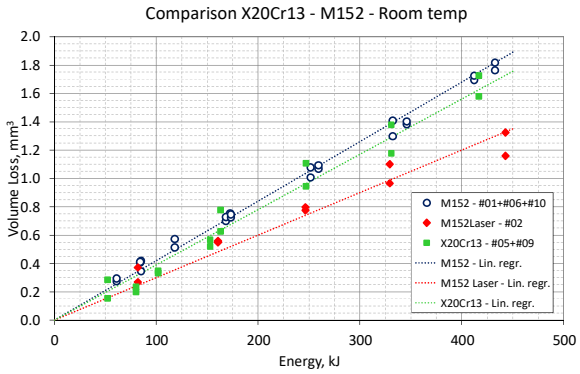

Fig. 6. Materials and heat treatment comparison, wear volume as a function accumulated dissipated energy.

Fig. 7 illustrates wear rate measured on plane surfaces versus slider for M152 and X20Cr13.

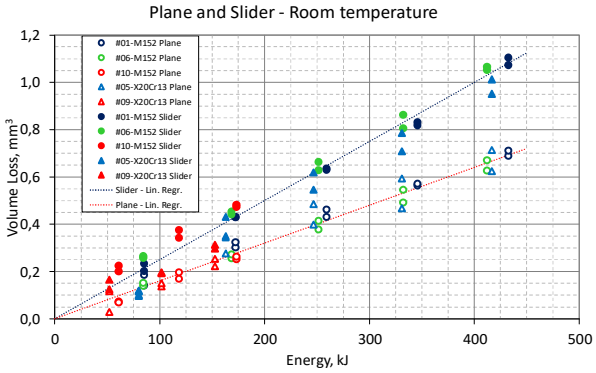

Fig. 7. Plan/slider comparison, wear volume as a function accumulated dissipated energy (a) M152; (b) X20Cr13.

In this figure the volume measurements made on the plane specimens (Fig. 3) were reported with solid markers (circular for the M152 and triangular for X20Cr13) while the measurements on the sliders were reported using empty markers (circular for the M152 and triangular for XCr13). The colours identify only the ID of the experiment. The first consideration is that the difference of wear rate between M152 and X20Cr13 observed in Fig. 6 can essentially be attributed to the sliders. The reason is that wear rate of the plane is substantially the same for both steels. On the other hand, the wear rate of the X20Cr13 sliders is lower than M152 sliders. The second and more evident consideration is that the plane specimens have a wear rate that is much lower than the sliders. This result means that the surface completely in contact (slider) shows a higher wear rate than the surface partially in contact (plane). Moreover, there is no difference between plane and slider surfaces along the fretting direction, the materials were the same with the same heat treatment and both type of specimens were obtained by same type of fabrication process. It seems that the part of the surface which has no contact (transversal to the fretting direction) has an influence on the wear rate. The fraction of the area without contact seems to reduce the wear rate of the surface fraction which is in contact with the slider. In other words, it seems a sort of surface integrity question. The fabrication process of the slider reduces the tribological properties more than the same type of fabrication process applied to the flat surface.

The effect of the temperature on X20Cr13 is illustrated in figure Fig. 8. The figure compares the wear volume by fretting process at RT with those at temperature of 150 °C with and without laser quenching. It is evident that the wear rate at 150 °C drastically decreases if compared with the RT.

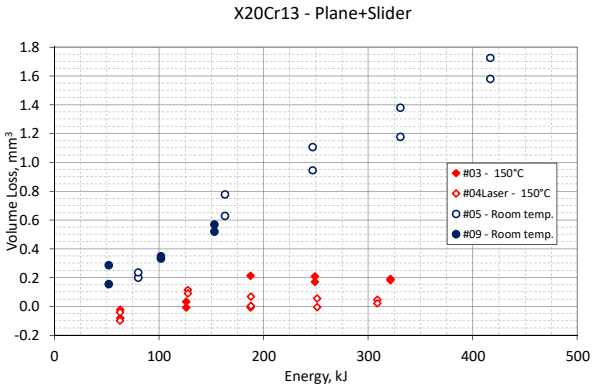

Fig. 8. Wear volume as a function accumulated dissipated energy at different temperatures.

The beneficial effect of the laser quenching process on wear rate is confirmed at the temperature of 150 °C if the dissipated energy is higher than 175 kJ. Under this threshold energy, the heat treatment seems to have no important influence.

The dissipated energy at 150 °C is lower than that at RT. Moreover, the laser quenched specimens show the lowest dissipated energy. This energy is slightly lower than the dissipated energy by specimens without laser quenching. Considering that the number of fretting cycles at RT was the same than at 150 °C, this means that the area of the hysteresis loops decreases, and consequently the friction coefficient decreases as the stroke is the same. Thus, there is a softening effect of the contact tangential force.

The temperatures of the contact interfaces were measured also during fretting experiments performed at RT by means of a thermocouple placed in the central position along the fretting direction at the distance of 1 mm from the contact interfaces [13]. In general the temperature of the contact interface during the fretting process at RT can reach about 60 – 70 °C for these geometries and process parameters. The maximum temperatures measured by thermocouple during the fretting process shown in Fig. 8 were 61 °C for the tribocouple #05 and 61 °C for the #05. Fig. 9 shows temperature increment of contact surface and dissipated energy per cycles measured at different fretting cycle. The temperature increment had the RT as a reference initial temperature. It was 22 °C for the experiment #05 and 27 °C for the #09. The dissipated energy per cycle should not be confused with the sum of the energy dissipated from each fretting cycles (accumulated dissipated energy) used before.

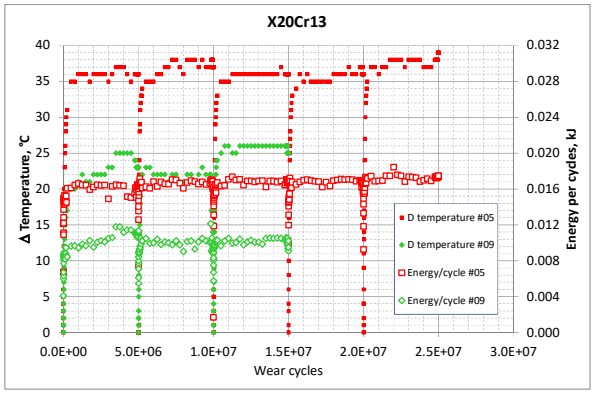

Fig. 9. Dissipated energy per cycle and contact temperature variation with reference to the room temperatures (22 °C for #05 and 27 °C for #09).

Fig. 9 evidences the coherence between the temperature increment and the dissipated energy per cycle. Substantially energy and temperature have the same evolution as a function of the number of fretting cycles. Tests were stopped and restarted every 5×10^6 cycle, consequently the temperature increment started from zero and reached the thermal regime when the dissipated energy balanced the heat transferred to the external environment. The initial increase in energy per cycle and consequently in temperature is due to the evolution of the sliding amplitude. This is regulated by the test rig control software to reach the target displacement stroke as soon as possible. Considering that the dissipated energy per cycle is strictly related to the stroke, a few cycles are necessary to reach the target displacement stroke and consequently the thermal regime. Moreover, from Fig. 9 it also evident that during tests performed at RT the contact temperature is higher (60 ÷ 70 °C) than RT. This is a direct consequence of the energy dissipated by friction. In other words, the real temperature difference between the tests was about 80 ÷ 90 °C (≅ 150 - 60 ÷ 70). This small temperature difference has a negligible effect on the mechanical properties of the analysed stainless steel, particularly at low temperature (150 °C). In contrast, the wear rate drastically decreases (Fig. 8). This small variation of the mechanical properties induces a drastic variation of fretting wear behaviour and suggests that there may be a transition state activated by an increasing in temperature. A large amount of literature, a representative list of works is reported in [19]-[25], is available on the severe-mild wear transition of steels. Typically, steels show a transition between severe to mild wear at temperature of about 80-220°C: beyond this temperature the fretting wear rate shows a sharp decreasing. The transition temperature seems to

depend on the steel type: it was found 80 °C for the S45C/S45C and 200 °C for SUS304/SUS304 in [21], 220 °C for M152/A286 in [22] and 85 °C for super-CMV/super-CMV in [23]. These transition temperature evokes a similar temperature for similar α-γ steel structures, in fact S45C, M152 and super-CMV have a α-structure while SUS304, A286 have γ-structure. In other words, the transition temperature seems to be about 80 °C for the alloy wit α-structure and about 200 °C for the γ-structure. Early works [19]-[21] associated this transition to the change in chemical composition and oxidation law of the oxides film built-up during the fretting process on the mating surfaces. The composition evolves from α-Fe_2O_3 to Fe_3O_4 while the oxide layer growth changes from logarithmic to parabolic grown. In [22] and [23] the transition is explained in terms of accumulations of debris retained inside the wear groove that leads to the formation of a stable-load bearing bed. This debris bed is due to the tribo-sintering process described in [24], [25] and evolves towards a glaze-layer as a consequence of a further temperature increasing. In [22] the transition occurs at about 210 °C and the glaze-layer is completely formed at 285 °C; in [23] the transition ensues at 85 °C and the glaze-layer is formed at 150 °C. According to this evidence, the severe-mild wear transition is usually located at the temperature of activation of the glaze-layer. However, the variation of temperature required by the wear rate transition is much lower than the variation of temperature required by the formation of the glaze-layer [22], [23]. Because of an increasing in temperature, the glaze-layer formation seems to be more gradual of the severe-mild wear transition. On the other hand, the glaze-layer formation explains the typical progressive reduction of the friction coefficient as a function of temperature reported in [12], [13], [22], [23]. This motivation seems to be less exhaustive if it refers to the wear rate transition. The reason is that the wear rate transition is very sharp while the sintering process of debris as a function of temperature is a gradual phenomenon. These considerations suggest the hypotheses that the evolution of the oxides layers by tribo-sintering process is coupled with a change of the damage mechanism from brittle to ductile. A brittle ductile transition may change significantly the production of debris by fretting process. Usually the α-structure shows brittle-ductile transition while γ-structure exhibit a ductile behaviour. Thus, when oxides with α-structure are predominant the damage mechanism could be brittle while when oxides with γ-structure are predominant the damage mechanism is ductile. The hypothesis is also compatible with the change of transition temperature of α-γ structures. In any case future research should verify this hypothesis of transition.

4. Conclusion

An experimental campaign was performed to investigate the fretting wear mechanism and wear evolution of the typical materials used for blades in low-pressure stages in steam turbines. The test parameters were representative of the typical operating conditions. A high-precision test rig with free approach of flat on flat contact surfaces was used in order to have rigorous measurements of wear evolution. Fretting experiments were not affected by imprecisions due to the assembling-reassembling of specimens and test rig compliance. Wear volume measurements as a function of wear cycles and dissipated energy were performed considering the roughness of the contact surfaces. The influences of normal load, material, heat treatment, surface integrity and temperature were illustrated. A wear rate as a function of the dissipated energy was found independent from the normal load. The analysed steels showed that the wear rate was far influenced by heat treatment than by the steel type. The beneficial effect of laser quenching was observed. The novel effect of the surface integrity has been highlighted. The surface integrity seems to play an important role and the plane surface shows a wear rate of about 60% of the wear rate of the sliders. During the fretting process at room temperature, the contact surface temperature increased up to 60-70 °C, due to the heat generated during the wear process. The comparison of experiments conducted at room and low temperature (150 °C) showed that a small variation of the test temperature originated a drastic variation of the wear rate. In other words, the same wear mechanism, adhesion and abrasion respectively in stick and gross slip condition, originated very different results, in terms of wear volume, due to a small softening effect of the material. This behaviour suggests a novel interpretation in terms of brittle-ductile transition of the oxides layers formed on the contact interfaces.

References

[1] T. Berruti, C.M. Firrone, M. Pizzolante, M.M. Gola, Fatigue damage prevention on turbine blades: Study of underplatform damper shape. Key Eng. Mater. 347 (**2007**) 159–164.

[2] G. Rigosi, G. Battiato, T.M. Berruti, Synchronous vibration parameters identification by tip timing measurements, Mechanics Research Communications 79 (**2017**) 7–14, DOI: 10.1016/j.mechrescom.2016.10.006.

[3] R. Ebara, Corrosion fatigue phenomena learned from failure analysis, Engineering Failure Analysis 13 (2006) 516–525.
[4] R. Ebara, Corrosion fatigue crack initiation in 12% chromium stainless steel, Materials Science and Engineering A 468–470 (2007) 109–113.
[5] Z. Mazur, R. García-Illescas, J. Porcayo-Calderón, Last stage blades failure analysis of a 28 MW geothermal turbine, Engineering Failure Analysis 16 (2009) 1020-1032.
[6] N. K. Mukhopadhyay, S. Ghosh Chowdhury, G. Das, I. Chattoraj, S. K. Das, D. K. Bhattacharya, An investigation of the failure of low pressure steam turbine blades, Engineering Failure Analysis 5 (1998) 181-193.
[7] C.R.F. Azevedo, A. Sinátora, Erosion-fatigue of steam turbine blades, Engineering Failure Analysis 16 (2009) 2290–2303.
[8] D. Botto, M. Umer, A novel test rig to investigate under-platform damper dynamics, Mechanical Systems and Signal Processing 100 (2018) 344-359.
[9] D. Botto, C. Gastaldi, M.M Gola, M. Umer, An Experimental Investigation of the Dynamics of a Blade with Two Under-Platform Dampers, J. Eng. Gas. Turbines Power-Trans. ASME 140(3) (2018) 032504, DOI: 10.1115/1.4037865.
[10] C.M. Firrone, T.M. Berruti, M.M. Gola, On force control of an engine order-type excitation applied to a bladed disk with underplatform dampers, J. Vib. Acoust. 135(4) (**2013**) 041103, DOI: 10.1115/1.4023899.
[11] M. Lavella, D. Botto, Fretting wear characterization by point contact of nickel superalloy interfaces, Wear 271 (2011) 1543–1551, DOI: 10.1016/J.wear.2011.01.064.
[12] Botto, D.; Lavella, M. High temperature tribological study of cobalt-based coatings reinforced whit different percentages of alumina, *Wear,* 2014, 318, 89–97, DOI: 10.1016/j.wear.2014.06.024.
[13] M. Lavella, Contact Properties and Wear Behaviour of Nickel Based Superalloy René 80, Metals 6 (7) (2016) 159, DOI: 10.3390/met6070159.
[14] M. Lavella, D. Botto, M.M. Gola, Design of a high-precision, flat-on-flat fretting test apparatus with high temperature capability, Wear 302 (2013) 1073–1081, DOI: 10.1016/j.wear.2013.01.066.
[15] M. Lavella, D. Botto, M.M Gola, Test rig for wear and contact parameters extraction for flat-on-flat contact surfaces, ASME/STLE 2011 International Joint Tribology Conference,

IJTC 2011, Los Angeles, CA, United States, 24-26 October 2011, DOI: 10.1115/IJTC2011-61234.

[16] S.R. Pearson, P.H. Shipway, Is the wear coefficient dependent upon slip amplitude in fretting? Vingsbo and Söderberg revisited, Wear 330-331 (2015) 93–102.

[17] S. Fouvry, P. Kapsa, L. Vincent, Analysis of sliding behavior for fretting loadings: determination of transaction criteria, Wear 185 (1995) 35–46.

[18] Botto, D.; Lavella, M. A numerical method to solve the normal and tangential contact problem of elastic bodies, *Wear,* 2015, 330-331, 629–635, DOI: 10.1016/j.wear.2015.02.046.

[19] P.L. Hurricks, The fretting wear of mild steel from room temperature to 200 °C, Wear 19 (1972) 207–229.

[20] P.L. Hurricks, The fretting wear of mild steel from 200 °C to 500 °C, Wear 30 (1974) 189–212.

[21] T. Kayaba, A. Iwabuchi, The fretting wear of 0045% C steel and Austenitic stainless steel from 20 to 650 °C in air, Wear 74 (1981) 229–245.

[22] R. Rybiak, S. Fouvry, B. Bonnet, Fretting wear of stainless steels under variable temperature conditions: introduction of a 'composite' wear law, Wear 268 (2010) 413–423.

[23] S.R. Pearson, P.H. Shipway, J.O. Abere, R.A.A. Hewitt, The effect of temperature on wear and friction of a high strength steel in fretting, Wear 303 (2013) 622–631.

[24] H. Kato, Severe-mild wear transition by supply of oxide particles on sliding surfaces, Wear 255 (2003) 426–429.

[25] H. Kato, K. Komai, Tribofilm formation and mild wear by tribo-sintering of nanometer-sized oxide particles on rubbing steel surfaces, Wear 262 (2007) 36–41.